International Journal of Research in Medical and Basic Sciences
Volume 6 Issue 12, December 2020 ISSN: 2455-2569 Impact Factor: 5.433
Journal Homepage: http://mbsresearch.com, Email: mbsresearchp@gmail.com
Double-Blind Peer Reviewed Refereed Open Access International Journal

Ultra flexible nanocarrier for enhanced the ocular delivery of quercetin in management of maccular ordema

Sahu Seema*, Shah Gulab Chand, Manigauha Ashish, Gupta Vandana**
***MITTAL INSTITUTE OF PHARMACY Opposite to Bhopal Memorial Hospital And Research Center (BMHRC) Nbibagh, Karond, Bhopal- 462038 (M.P)**
****School of Biotechnology RGPV BHOPAL, 462033 (M.P)**
Email: Coropondence Auther*gulab777@gmail.com

ABSTRACT

Quercetin (Que) and its derivatives are naturally taking place phytochemicals with promising bioactive belongings. The antidiabetic, antiinflammatory, antioxidant, antimicrobial, anti-Alzheimer's, antiarthritic, cardiovascular, and wound-healing possessions of Que have been extensively investigated, as well as its anticancer commotion against different cancer cell lines has been newly reported. Que and its derivatives are found predominantly in the Western starve yourself, and people might benefit from their defensive effect just by taking them via diets or as a food enhancement. Bioavailability-related drug-delivery systems of Que have also been markedly exploited, and Que nanoparticles become visible as a promising proposal to enhance their bioavailability. The present review aims to make available a brief overview of the therapeutic things, new insights, and forthcoming perspectives of Que. Plants and plant parts are used for its aroma, flavor, or therapeutic properties. There are a number of recompense associated with using plants and plant phytoconstituents as contrasting to pharmaceutical merchandise.

Key Words: Quercetin (Que), Ultraviolet(UV), Thermogravimetric Analysis (TGA), Solid lipid Nanoparticle (SLN), Polyethylene Oxide (PEO), Isotonic Phosphate Buffer Saline (IPBS)

1. INTRODUCTION

With increased age comes declining health conditions and increased prevalence in diseases. Included in this broad category is the deterioration of vision due to a variety of factors contributing to a number of ophthalmic diseases. These diseases can include age-related macular degeneration, cataracts, diabetic retinopathy, and glaucoma. According to statistics by the National Eye Institute, several millions of people above the age of forty are affected by one of these conditions. From the total population of those above age forty in the 2010 U.S. Census (n = 142,648,393), 36,883,997 adults suffered from vision impairment due to all of the ophthalmic diseases listed above combined (NEI "Prevalence", 2016). This is approximately over a quarter (25.9%) of adults over age forty who are affected with vision impairment. As age increases, the prevalence rates of all vision impairment also increase, rising significantly around ages 75-79 in all ethnicities, as shown in Figure 1.

International Journal of Research in Medical and Basic Sciences
Volume 6 Issue 12, December 2020 ISSN: 2455-2569 Impact Factor: 5.433
Journal Homepage: http://mbsresearch.com, Email: mbsresearchp@gmail.com
Double-Blind Peer Reviewed Refereed Open Access International Journal

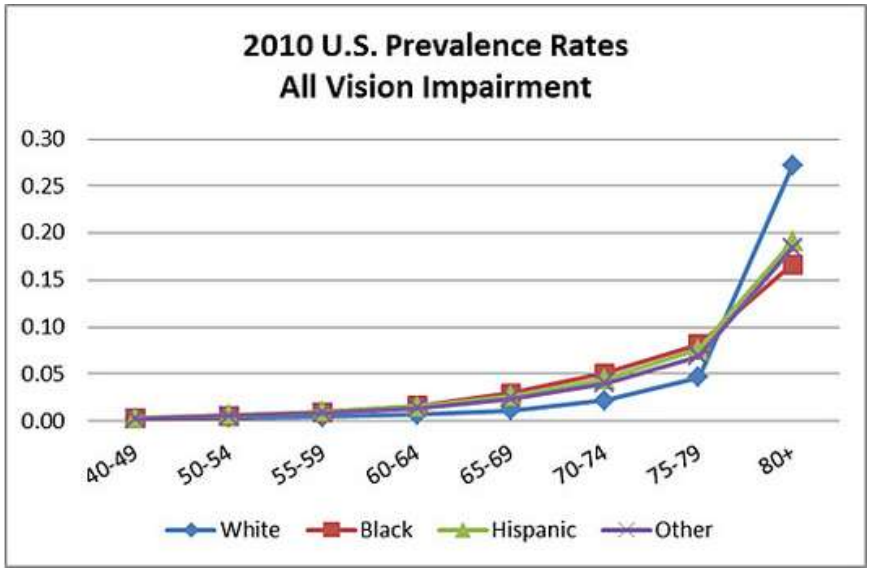

Figure 1. 2010 U.S. Prevalence Rates: All Vision Impairment

Source: National Eye Institute. All Vision Impairment. Available at: https://nei.nih.gov/eyedata/vision_impaired#1. Accessed March 27, 2020.

Over the course of ten years, starting from the year 2000, the prevalence of vision impairment has increased by almost 130% (NEI "Vision", 2016). These trends are expected to continue with each subsequent year so that by the year 2030, there will be almost a two-fold increase in prevalence of vision impairment compared to that in 2010, and by 2050, there will be more than a 3-fold increase in prevalence, as shown in Table 1 and Figure: 2.

Table 1. Table Projections for Vision Impairment (2010-2030-2050)

Year	All	White	Black	Hispanic	Other
2010	4,195,966	3,398,977	330,644	290,781	175,564
2030	7,169,680	5,277,689	618,110	840,497	433,383
2050	13,026,870	9,019,189	1,047,986	2,000,853	958,842
Total Population	**142,648,393**	**103,846,437**	**15,190,777**	**14,901,369**	**8,709,810**

Source: National Eye Institute. Vision Impairment Tables. Available at: https://nei.nih.gov/eyedata/vision_impaired/tables. Accessed March 27, 2020.

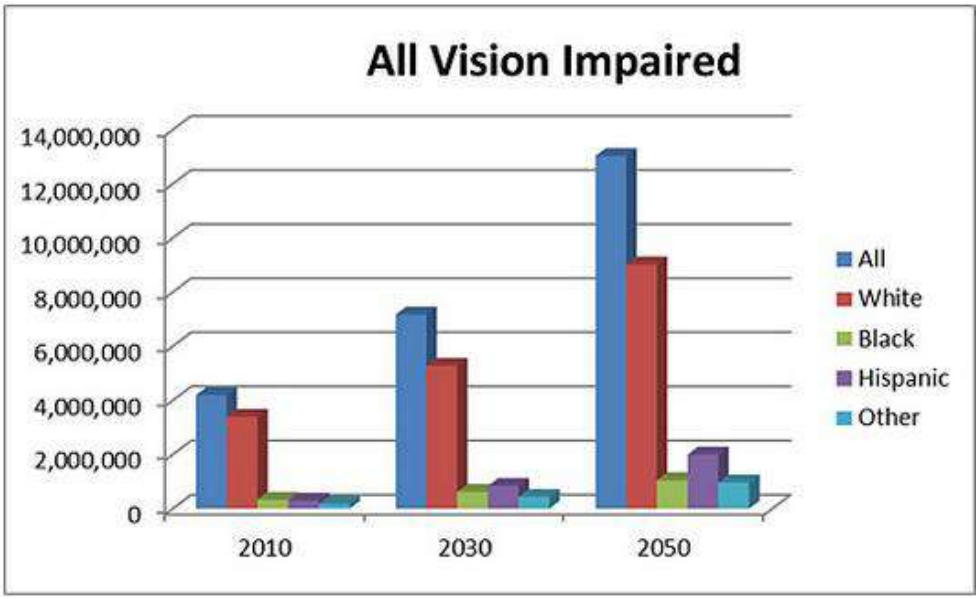

Figure:2 Chart Projections for Vision Impairment (2010-2030-2050)

Source: National Eye Institute. All Vision Impairment. Available at: https://nei.nih.gov/eyedata/vision_impaired#1. Accessed March 27, 2020.

One cause of vision impairment is due to uncontrolled exposure to reactive oxidative species, or ROS. These are species that are produced naturally in the body as a byproduct of adenosine triphosphate, or ATP, production, the energy source that is used for every day function and processes (Prunty, 2015). They are free radicals that contain oxygen and are the most common type produced in tissues (NCI, 2014). They can affect cells by damaging important cellular components, such as DNA, proteins, and membranes. The mitochondria, an efficient organelle found abundantly in the body's cells and tissues, produce the largest quantities of ROS as it is the largest contributor to ATP synthesis (90% of the body's energy) [UMDF, 2017]. The body has natural antioxidant mechanisms to protect against ROS, but when ROS are overproduced, these mechanisms are overwhelmed (Prunty, 2015). This leads to oxidative stress cascades on cells and tissues, which causes them to become damaged and eventually die off. In the eye,

ROS damage the cells of the retina, which plays an important role in converting visual images into electrical impulses for the brain to interpret. As the photoreceptor cells of the retina die off, vision worsens as the eye has less capability to convert those images to impulses. The longer the period of exposure to ROS, the more damage is done to the retina. Prolonged damage to the retina exacerbates retinal degradation and degeneration, further impairing vision and may even lead to permanent blindness. This is why as a person ages, their vision becomes progressively worse.

A protective measure against ROS is the use of antioxidant treatments. Antioxidants can be used to slow the rate of retinal degradation by counteracting damage from the reactive oxidative species. The body produces some antioxidants endogenously, but they can also be obtained outside of the body. They can be found in a variety of antioxidant-rich foods, such as fruits, leafy green vegetables, and grains, and can also be obtained through dietary supplements. These include carotenoids like beta-carotene, lycopene, and vitamins A, C, and E (NCI, 2014). There are a variety of substances that act as antioxidants, like the ones mentioned before, in addition to glutathione, coenzyme Q10, lipoic acid, flavonoids, phenols, polyphenols, phytoestrogens, etc., all having different properties and roles against ROS (Harvard, 2017). In the case of preventing retinal degradation to improve outcomes in terms of vision integrity and function, antioxidants can be employed to protect against the damage from reactive oxidative species. However, because of physiological barriers, antioxidants cannot simply be taken orally and expected to be able to reach its target, i.e. the retina, to enact its protection.

2. QUERCETIN

Quercetin, which has the chemical name of 2-(3,4-Dihydroxyphenyl)-3,5,7-trihydroxy-4*H*-1-benzopyran-4-one, is a bioflavonoid aglycone, specifically of the flavonol subclass, meaning that it has a 3-hydroxyflavone backbone and lacks attached sugars, as shown in Figure 3 (Kelly, 2011).

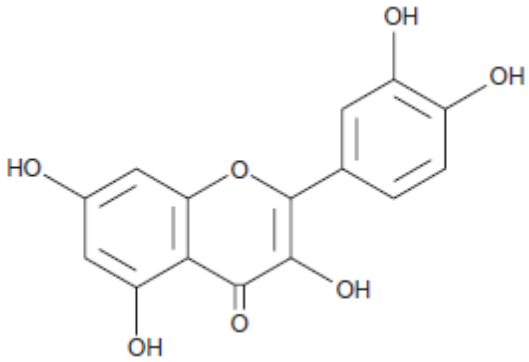

Figure 3. Quercetin Structure

It is a crystalline solid that has a bright citron yellow color. It is lipophilic and hydrophobic in nature so its solubility in water is poor to nonexistent (poor in hot water and entirely insoluble in cold water). A way to improve its solubility in water is to convert it to a glycoside. This can be done by replacing one of the hydroxyl groups, commonly the one at position 3, with a glycosyl group, which can be any sugar such as glucose, rhamnose, or rutinose (see Figure 6). A glycoside group at position 3 is known as isoquercitin. The addition of a glycosyl group changes the chemical properties of the drug, including solubility, absorption, and *in vivo* effects. Specifically, the addition of the glycosyl group increases the water solubility of quercetin.

3. MATERIALS:

Quercetin was purchased from Tocris Bioscience. Glycerol monostearate and Compritol ATO 888® were graciously donated by Gattefossé. Miglyol 812® was purchased from Dr Reddy lab Hyderabad India . Tween 80 and methyl-beta-cyclodextrin were purchased from Acros Organic. Poloxamer 188 was purchased from Spectrum. Glycerin was purchased from PCCA. Acetonitrile and dimethyl sulfoxide were purchased from Fisher Chemical. Whole rabbit eye globes were purchased from Pel-Freez Biologics. The rabbit eye globes were dissected in lab to collect the corneas for use in the permeability studies.

4. METHODS:

A. Solid Lipid Nanoparticles:

Quercetin solid lipid nanoparticles, or SLNs, were prepared by probe sonication method. The lipid phase was prepared with a solid lipid (0.7% w/v Glycerol monostearate) in combination with 1.3% w/v Compritol ATO 888® and heated on a hot plate at 80oC. Quercetin was dissolved in 100 µL of dimethyl sulfoxide and added to 2.25% w/v glycerin. This mixture was added to the melted lipid phase. The aqueous phase was prepared using 0.75% w/v Tween 80®, Poloxomer 188®, and filtered water and heated on the hot plate at 80oC. The aqueous phase was then added to the lipid phase while stirring at 600 rpm for 2 minutes. The final concentration of quercetin was 0.1% w/v. The premix was homogenized with an Ultra-Turrax® at 16,000 rpm for 3 minutes to form a coarse emulsion. This coarse emulsion was then subjected to probe sonication at a 15-second pulse rate for 3 minutes. The final emulsion was allowed to cool to form the nanoparticles.

B. Nanostructured Lipid Carriers:

Quercetin nanostructured lipid carriers, or NLCs, were also prepared by probe sonication method. The method is almost exactly the same as that for the SLN formulation, except that the lipid phase was prepared with a liquid lipid (0.7% w/v Miglyol 812®) in combination with 1.3% w/v Compritol ATO 888®, which was then heated on a hot plate at 80oC. Quercetin was dissolved in 100 µL of dimethyl sulfoxide and added to 2.25% w/v glycerin. This mixture was then added to the melted lipid phase. The aqueous phase was prepared using 0.75% w/v Tween 80®, Poloxomer 188®, and filtered water and heated on the hot plate at 80oC. The aqueous phase was added to the lipid phase while stirring at 600 rpm for 2 minutes. The final concentration of quercetin was 0.1% w/v. The premix was homogenized with an Ultra-Turrax® at 16,000 rpm for 3 minutes to form a coarse emulsion, which was then subjected to probe sonication at a 15-second pulse rate for 3 minutes. The final emulsion was allowed to cool to form the nanoparticles.

C. Hot Melt Cast Films:

Quercetin films were prepared by melt-cast method. Polyethylene oxide N10 was used as the matrix forming polymer. Quercetin and PEO N10 were mixed via geometric dilution to prepare the physical mixture. The drug load in the film was 10% w/w. A 10 mm die was placed over a brass plate and heated on a hot plate at 75°C for at least one minute. The physical mixture was poured into the center of the die and compressed for a few seconds to form a flat matrix surface. The film was heated on the hot plate for an additional minute so that the mixture was completely melted and then removed to cool. When completely cooled, the film was cut to collect samples that weighed approximately 8 mg each.

D. Characterization of Nanoparticles:

Mobile phase of acetonitrile**:**water (ACN:H2O, 40:60) was prepared. Quercetin was dissolved in dimethyl sulfoxide (DMSO) to make a 1 mg/mL stock solution for the standards. Varying volumes of the stock solution were diluted with the mobile phase to make standards of the following concentrations: 1 µg, 2 µg, 5 µg, 10 µg, and 20 µg. The standards were analyzed using UV analysis at a wavelength of 369 nm to determine the light absorbance trend, or calibration curve, of quercetin to which the nanoparticle emulsions will be compared. The SLN and NLC formulations were diluted 500 times with purified water and analyzed using a zetasizer (Malvern Instruments, Ltd.) to determine the size, polydispersity index, and zeta potential of the particles. The goal was to have small particle sizes, low polydispersity index, and high magnitude of zeta potential for the most stable and homogeneous formulation.

Entrapment efficiency, which is a measure of how much drug is entrapped in the nanoparticles, was performed by centrifuging 500 µL of each formulation with a filter for 15 minutes. 100 µL of the centrifuged filtrate was drawn, diluted with 900 µL of the mobile phase, and then vortexed to ensure thorough and homogeneous mixing. Assay was performed to determine quercetin content in the nanoparticles. For each formulation, 100 µL of formulation were added to 900 µL of a mixture of DMSO

and methanol (50:50) and sonicated for 10 minutes. After sonication, the mixture was centrifuged for 15 minutes. From this, 100 µL of the supernatant was drawn and diluted with 900 µL of the mobile phase before being vortexed to ensure thorough and homogeneous mixing. All samples collected from entrapment efficiency and assays were analyzed in triplicates using HPLC-UV method with a Kinetex® 5 µm EVO C18 100 Å LC column (250 x 4.6 mm).

E. Characterization of Films:

Mobile phase of acetonitrile**:**water (ACN:H2O, 40:60) was prepared. Quercetin was dissolved in dimethyl sulfoxide (DMSO) to make a 1 mg/mL stock solution for the standards. Varying volumes of the stock solution were diluted with acetonitrile to make standards of the following concentrations: 1 µg, 2 µg, 5 µg, 10 µg, and 20 µg. The standards were analyzed using UV analysis at a wavelength of 369 nm to determine the calibration curve of quercetin to which the film samples will be compared.

Samples of approximately 8 mg were cut from quercetin films and added to 2 mL of acetonitrile. This mixture was then sonicated for 5 minutes until the film was completely dissolved. After sonication, the stock was diluted by a factor of 20. All samples were collected and analyzed in triplicates using UV analysis at a wavelength of 369 nm.

F. Permeability Studies:

Release and permeability of quercetin from the nanoparticles were studied using a vertical dialysis cassette with a 10,000 Dalton MWCO membrane. Isotonic phosphate buffer saline, or IPBS, was made with 5% methyl-beta-cyclodextrin. IPBS served as the receiver medium. 18 mL of IPBS was filled into the vial, and 1 mL of formulation was filled into the cassette. Measurements were taken at 15, 30, 60, 90, 120, 150, and 180 minute time points, at which time 1 mL of the receiver medium was drawn and 1 mL of IPBS was added into the vial. All samples collected were analyzed in triplicates under HPLC-UV method.

Permeability of quercetin from NLCs and films was studied using fresh rabbit cornea in a side-by-side diffusion apparatus, maintained at 34°C using a circulating water bath. IPBS with 5% methyl-beta-cyclodextrin was made. Spectra/Por® membrane (10,000 Daltons MWCO) were cut and soaked in IPBS for 30 minutes. Side-by-side diffusion cells were set up so that the fresh rabbit cornea and Spectra/Por® membrane were sandwiched between the cells. For the film studies, the films were cut to approximately 45 mg and wetted with IPBS. They were then sandwiched between the rabbit cornea and Spectra/Por® membrane, in the following order: donor cell Spectra/Por® membrane quercetin film cornea recipient cell (see Figure 4).

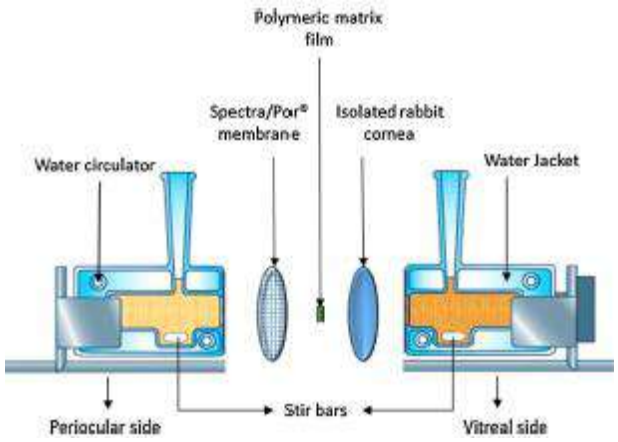

Figure 4. Side-by-Side Diffusion Apparatus Setup

Source: Adelli GR, Hingorani T, Punyamurthula N, et al. Evaluation of topical hesperetin matrix film for back-of-the-eye delivery. *European Journal of Pharmaceutics and Biopharmaceutics* 2015; 92:74-82.

Both the donor and recipient cells for the film studies were filled with 3.2 mL of IPBS. For the NLC formulations and the control, which was 3 mg of pure quercetin mixed with IPBS, 3.2 mL of each formulation were added into their respective donor cells, and 3.2 mL of IPBS were added to the recipient cells. Measurements were taken at 30, 60, 90, 120, 150, and 180 minute time points. After flushing a few

times to mix the receiver medium, 0.6 mL samples were drawn from the recipient cell, except for the films, for which samples were collected from both donor and recipient cells, and 0.6 mL of IPBS was added to the cells to replace the volume removed. The samples were analyzed in triplicates using UV analysis at a wavelength of 369 nm.

5. RESULT AND DISCUSSION

5.1 Characterizations of Nanoparticles and Films:

The solid lipid nanoparticles demonstrated an average particle size of 65.4 r.nm, polydispersity index of 0.29, and zeta potential of -12.3 mV. Assay and entrapment efficiency results were 78.4 ± 1.6% and 90.9 ± 0.3%, respectively. Drug release across the Spectra/Por® membrane was 33.3 ± 1.5%. These parameters are summarized below in Table 2. Particle size distribution is shown in Figure 5.

Table 2. Physicochemical Characterization of SLN Formulations

Parameters	Solid Lipid Nanoparticles
Particle Size (r.nm)	65.4
Polydispersity Index	0.29
Zeta Potential (mV)	-12.3
Assay	78.4 ± 1.6
Entrapment Efficiency	90.9 ± 0.3
% Release across Spectra/Por® Membrane	33.3 ± 1.5

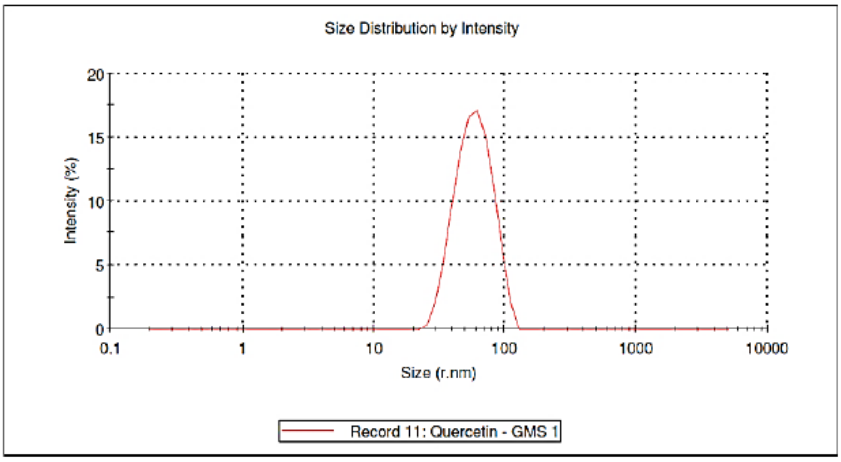

Figure 5. SLN Particle Size Distribution by Intensity

The nanostructured lipid carriers demonstrated an average particle size of 46.1 r.nm, polydispersity index of 0.18, and zeta potential of -16.2 mV. Assay and entrapment efficiency results were 86.6 ± 0.2% and 93.4 ± 0.1%, respectively. Drug release across the Spectra/Por® membrane was 47.1 ± 7.9%. These parameters are summarized below in Table 3, and particle size distribution is shown below in Figure 6. The comparison of the particle size distributions for the SLN and NLC formulations is shown below in Figure 7.

Table 3. Physicochemical Characterization of NLC Formulations

International Journal of Research in Medical and Basic Sciences
Volume 6 Issue 12, December 2020 ISSN: 2455-2569 Impact Factor: 5.433
Journal Homepage: http://mbsresearch.com, Email: mbsresearchp@gmail.com
Double-Blind Peer Reviewed Refereed Open Access International Journal

Parameters	Nanostructured Lipid Carriers
Particle Size (r.nm)	46.1
Polydispersity Index	0.18
Zeta Potential (mV)	-16.2
Assay	86.6 ± 0.2
Entrapment Efficiency	93.4 ± 0.1
% Release across Spectra/Por® Membrane	47.1 ± 7.9

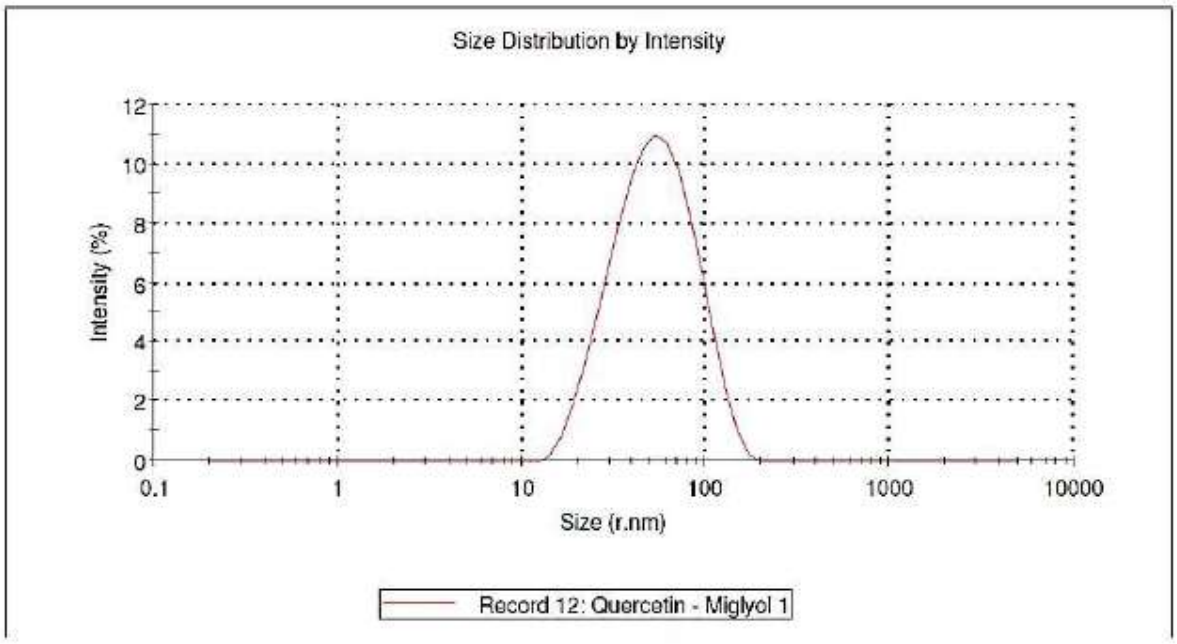

Figure 6. NLC Particle Size Distribution by Intensity

International Journal of Research in Medical and Basic Sciences
Volume 6 Issue 12, December 2020 ISSN: 2455-2569 Impact Factor: 5.433
Journal Homepage: http://mbsresearch.com, Email: mbsresearchp@gmail.com
Double-Blind Peer Reviewed Refereed Open Access International Journal

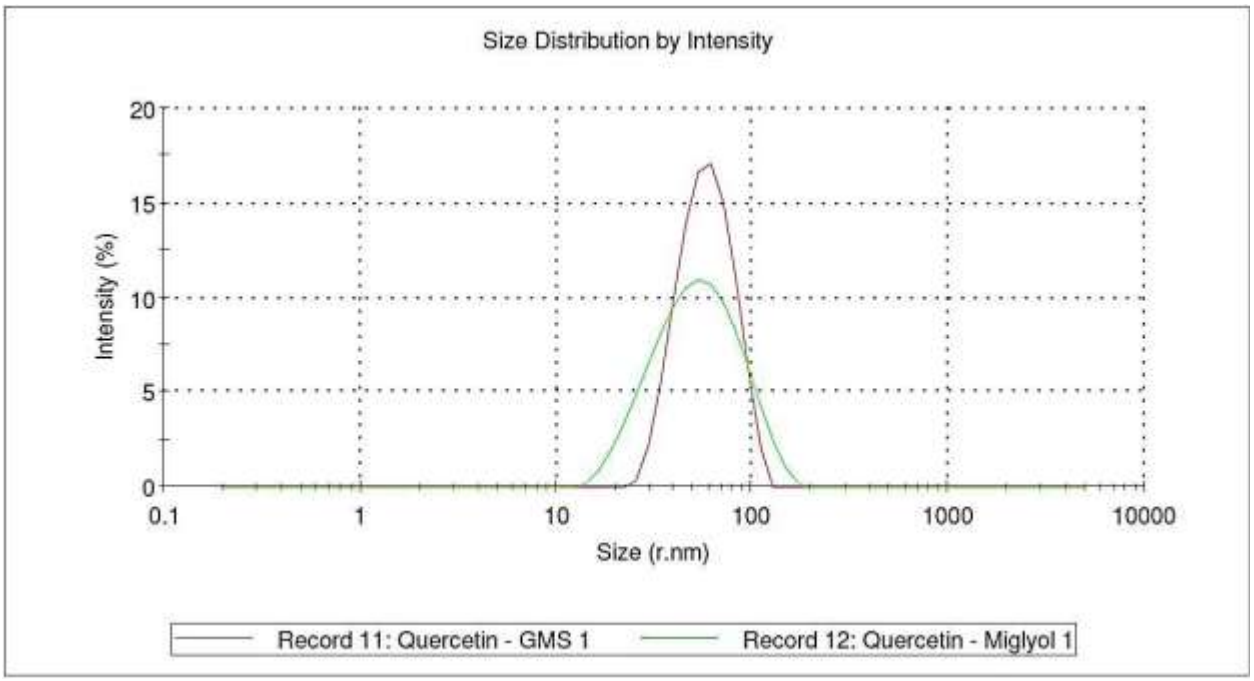

Figure 7. SLN vs. NLC Size Distributions by Intensity

Hot melt cast films demonstrated assay results of 76.3 ± 4.1%. Particle size, polydispersity index, zeta potential, and entrapment efficiency are parameters designed more for nanoparticle systems and were not evaluated with the hot melt cast films. Drug release across Spectra/Por® membranes was also not evaluated with the films.

5.2 Corneal Permeability Studies:

All samples were analyzed via UV analysis at a wavelength of 369 nm, at which the standard calibration curve had an R2 value of 0.9989. TGA data indicated that physical mixtures were stable under the utilized processing temperature. Permeability across the rabbit cornea for quercetin films, NLCs, and control are shown in Figures 8, 9, and 10, respectively.

International Journal of Research in Medical and Basic Sciences
Volume 6 Issue 12, December 2020 ISSN: 2455-2569 Impact Factor: 5.433
Journal Homepage: http://mbsresearch.com, Email: mbsresearchp@gmail.com
Double-Blind Peer Reviewed Refereed Open Access International Journal

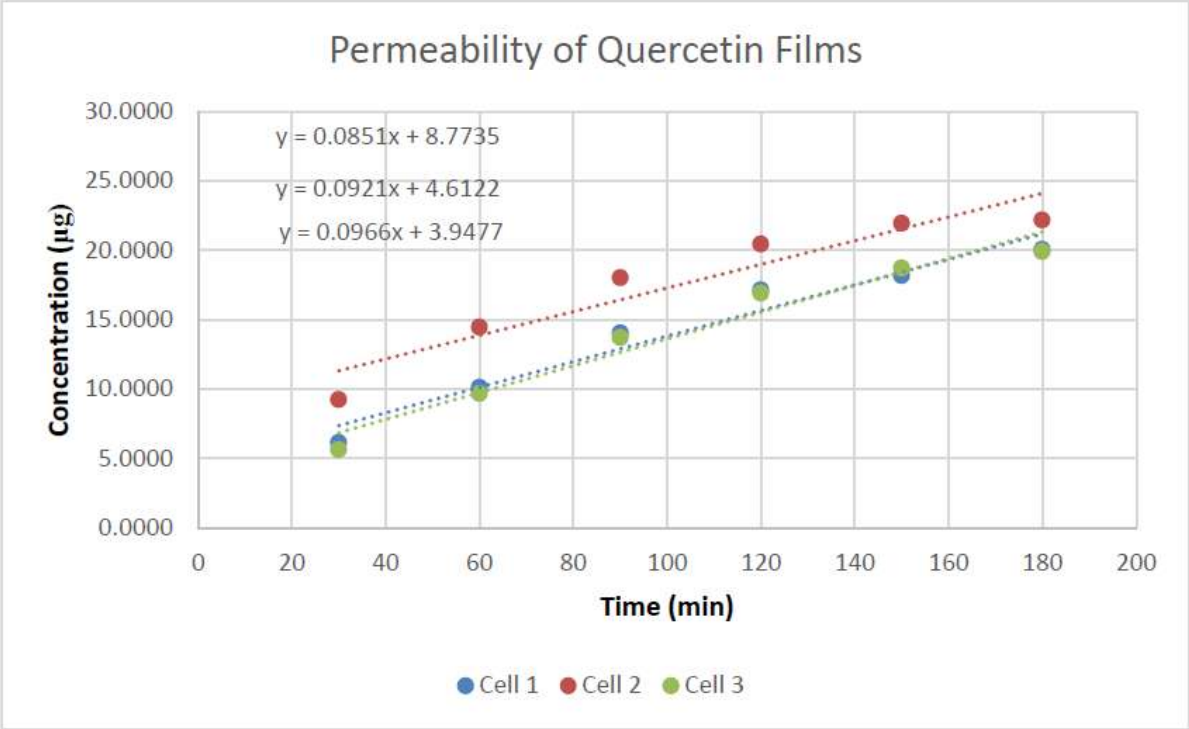

Figure 8. Permeability of Quercetin Films

International Journal of Research in Medical and Basic Sciences
Volume 6 Issue 12, December 2020 ISSN: 2455-2569 Impact Factor: 5.433
Journal Homepage: http://mbsresearch.com, Email: mbsresearchp@gmail.com
Double-Blind Peer Reviewed Refereed Open Access International Journal

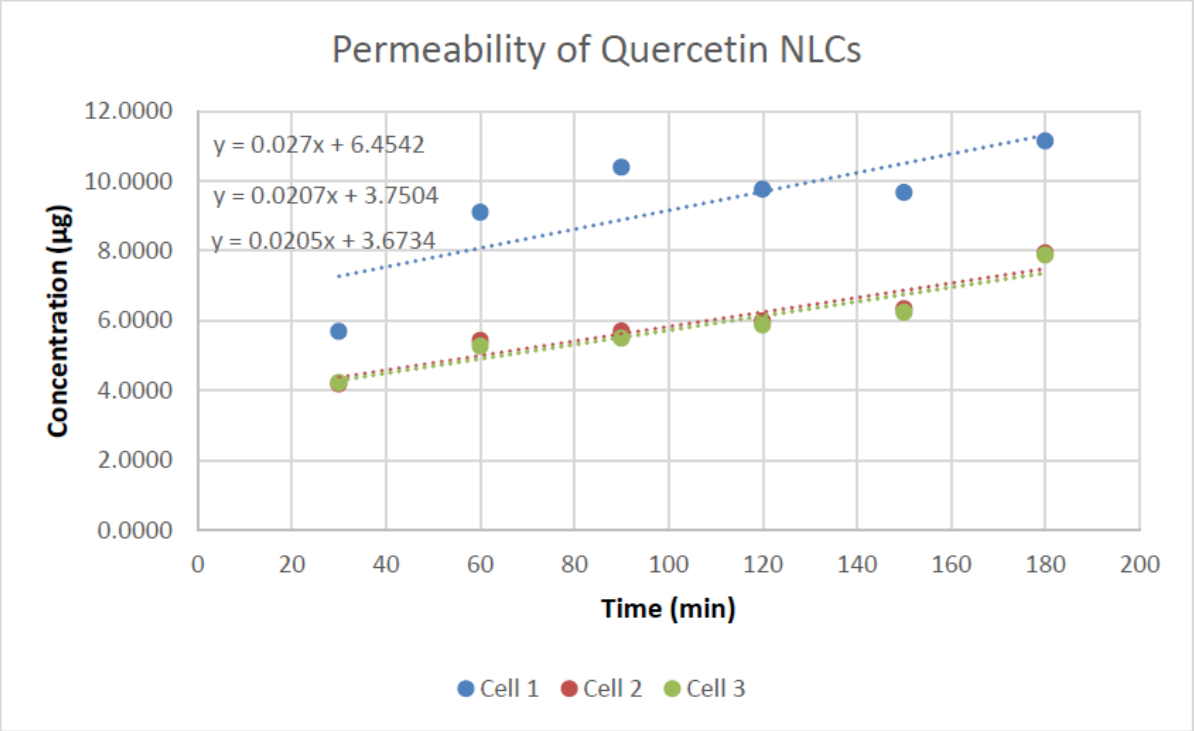

Figure 9. Permeability of Quercetin NLCs

International Journal of Research in Medical and Basic Sciences
Volume 6 Issue 12, December 2020 ISSN: 2455-2569 Impact Factor: 5.433
Journal Homepage: http://mbsresearch.com, Email: mbsresearchp@gmail.com
Double-Blind Peer Reviewed Refereed Open Access International Journal

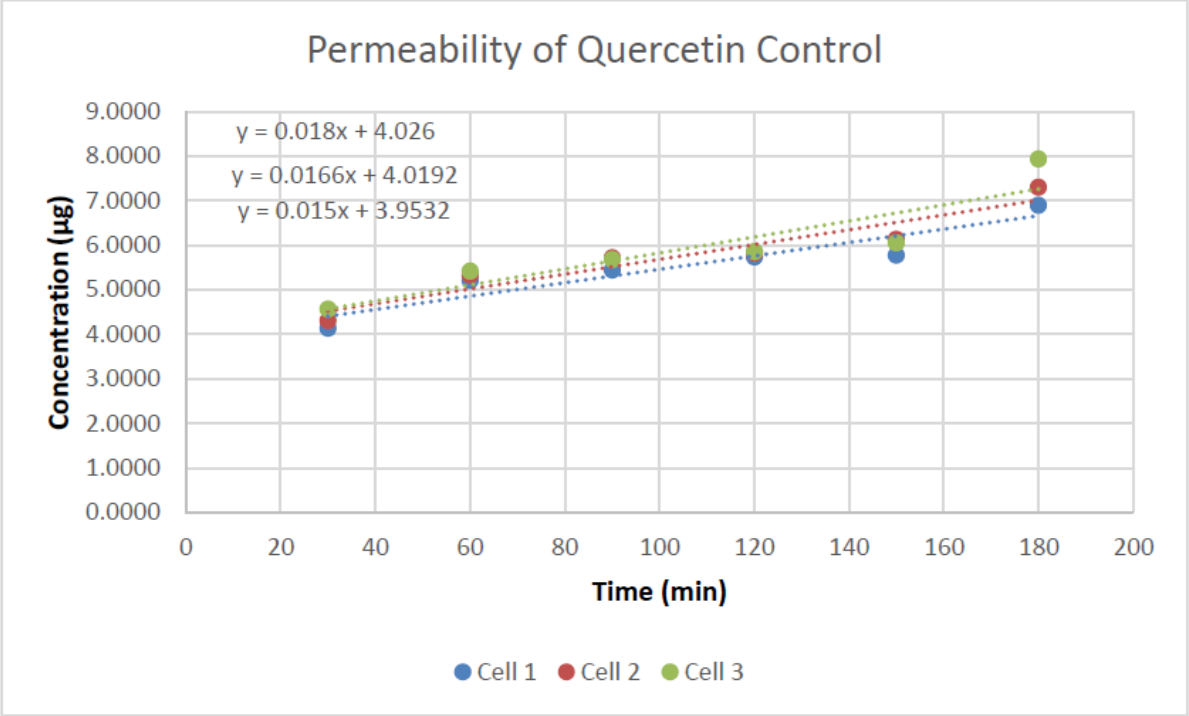

Figure 10. Permeability of Quercetin Control

The results from the permeability studies, in terms of rate, flux, and permeability, are summarized in Table 4 and Figure 11. Transcorneal flux, which is the amount of drug that crosses the cornea per minute per area squared (in this case, the area of the cornea is 0.636 cm), of quercetin control, NLCs, and films were 0.026 ± 0.002, 0.036 ± 0.006, and 0.144 ± 0.009, respectively. Permeability was calculated as flux normalized by assay.

Table 4. Results for Permeability Studies (Rate, Flux, Permeability)

	Rate (µg/min)	Flux (µg/min/cm^2)	Permeability X 10^6 (cm/sec)
Control	0.0165 ± 0.002	0.0260 ± 0.002	0.135 ± 0.012
NLCs	0.0227 ± 0.004	0.0357 ± 0.006	0.186 ± 0.030
Films	0.1435 ± 0.006	0.1435 ± 0.009	0.747 ± 0.047

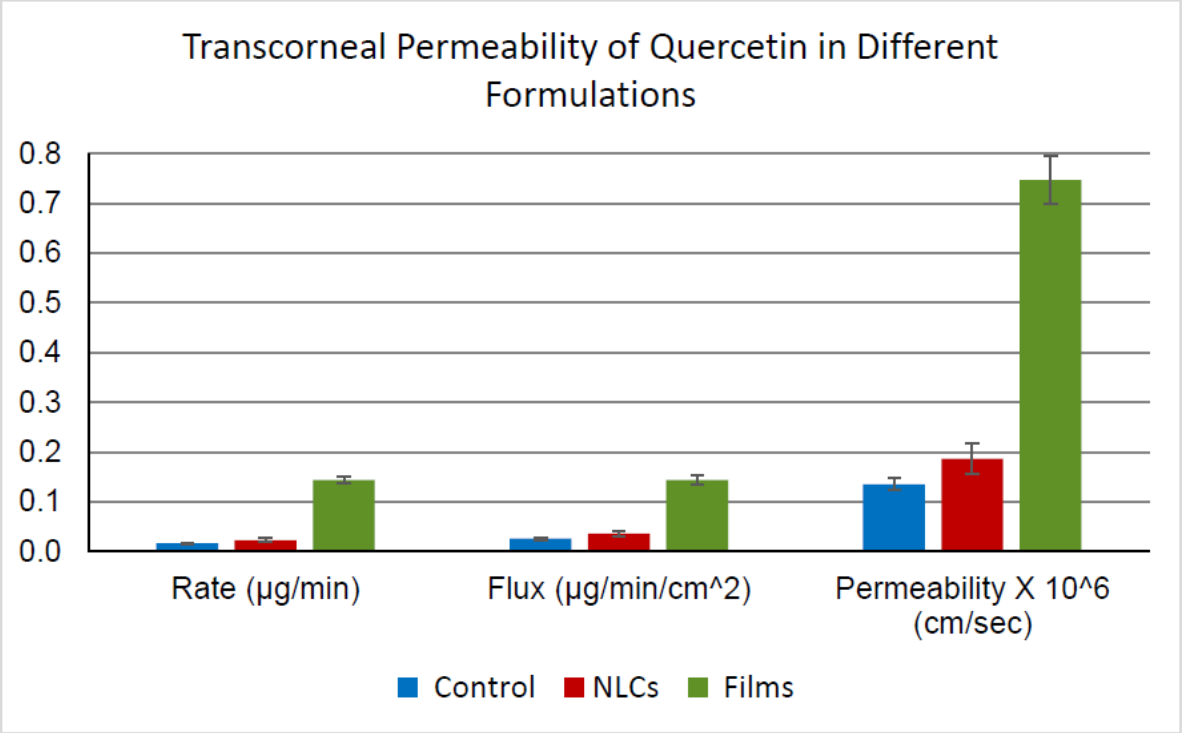

Figure 11. Transcorneal Permeability of Quercetin in Different Formulations

The goal parameters for the nanoparticle formulations were to have small particle sizes, low polydispersity index, and high magnitude of zeta potential. Both the solid lipid nanoparticles and the nanostructured lipid carriers successfully met and fit well within these goal parameters. Particle sizes for both formulations were well below 500 nm. The peak of the particle size distribution for the NLC

formulation was higher and narrower compared to the peak for the SLN formulation, as the intensity was noticeably greater and the particle sizes were less variable. Polydispersity indices for both were close to zero (0), which is the most ideal polydispersity index in order to have a completely uniform formulation. Zeta potentials for both were relatively high in magnitude as well (between -10 and -20 mV). Both entrapment efficiencies were at least 90% or higher. Drug releases across the Spectra/Por® membrane for both formulations, on the other hand, were relatively low (around 30-50%). When comparing assays for all three formulations (SLNs, NLCs, and films), film assay results were the lowest (by 2%), and NLCs were the highest (by about 8%), with SLNs in between the two. In all regards, the NLC formulation had better physicochemical characteristics compared to the SLN formulation. This is due to the nature of the lipid matrix shells of the nanoparticles. Because solid lipid nanoparticle formulations use only solid lipids, the matrix shells are completely solid and continuous, which has limited permeability. Not only does this affect how much drug can be encapsulated in the nanoparticles, but it also affects how the drug diffuses out of the nanoparticles. Specifically, this structure results in a relatively low drug load, limited drug release, and drug expulsion during storage. With nanostructured lipid carriers, on the other hand, the incorporation of a liquid lipid to the solid lipid matrix results in a disrupted and highly permeable nanoparticle shell. This structure allows for a higher drug load, greater drug release, and long term drug stability. Thus, from these differences (summarized in Figure 12), we would expect to see that the NLC formulation would show better characteristics than the SLN formulation, which it did.

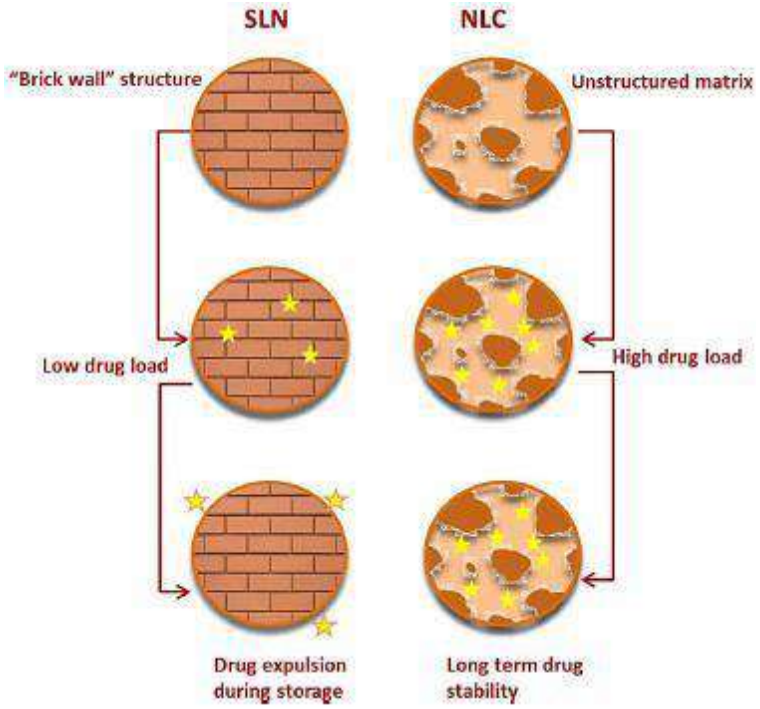

Figure 12. Advantages of NLC Structure over SLN Structure

Source: Beloqui A, Solinis MA, Rodríguez-Gascón A, Almeida AJ, Préat V. Nanostructured lipid carriers: promising drug delivery systems for future clinics. *Nanomedicine: Nanotechnology, Biology and Medicine* 2016; 12:143-161.

To compare how well quercetin permeates from the hot melt cast film across corneas as opposed to permeation from the nanoparticles, we used a control of pure quercetin in addition to the NLC formulation, which was chosen because it demonstrated better parameters and physicochemical characteristics compared to the SLNs. The three main parameters tested in the permeability studies were rate, flux, and permeability. Rate was determined by how much drug, in micrograms (μg), crossed the cornea from the donor to the receiver cells, per minute, with concentrations extrapolated from the calibration curve based on the absorbance of the samples. The rate of drug release permeation for the control was the slowest, and the rate for the films was the highest by a significant margin (7-14x higher),

with the rate of the NLCs in between the two. Flux was calculated as the amount of drug in micrograms that crosses the cornea per minute per area squared (area = 0.636 cm). Again, the flux for the control was the lowest, and the flux for the films was the highest by a good margin (4-5x higher). Flux for NLCs was in between the other two flux values. Lastly, permeability was calculated as flux normalized by assay and reported as centimeters per second. These results showed the same trends as with the other two parameters. The permeability of the control across the cornea was the lowest, the permeability of the drug from the NLCs was second highest, and the permeability of the drug from the films was the highest, once again by a good margin (4-6x higher). In total, both formulations (NLCs and films) were more successful compared to the control in drug permeability across the cornea. However, the hot melt cast film formulation showed significantly better parameters in all respects compared to both the control and the NLC formulation.

6. REFERENCES

Abraham M, Acree W. On the solubility of quercetin. *Journal of Molecular Liquids* [serial online]. September 1, 2014;197:157-159.

Adelli GR, Balguri S, Majumdar S. Effect of cyclodextrins on morphology and barrier characteristics of isolated rabbit corneas. *AAPS PharmSciTech* 2015;16:1220-1226.

Adelli GR, Hingorani T, Punyamurthula N, et al. Evaluation of topical hesperetin matrix film for back-of-the-eye delivery. *European Journal of Pharmaceutics and Biopharmaceutics* 2015; 92:74-82.

Aditya NP, Macedo AS, Doktorovova S, et al. Development and evaluation of lipid nanocarriers for quercetin delivery: A comparative study of solid lipid nanoparticles (sln), nanostructured lipid carriers (nlc), and lipid nanoemulsions (lne). *LWT – Food Science and Technology* 2014;59:115-121.

Balguri SP, Adelli GR, Majumdar S. Topical ophthalmic lipid nanoparticle formulations (sln,nlc) of indomethacin for delivery to the posterior segment ocular tissues. *European Journal of Pharmaceutics*

and Biopharmaceutics 2016; 109:224-235.

Beloqui A, Solinis MA, Rodríguez-Gascón A, Almeida AJ, Préat V. Nanostructured lipid carriers: promising drug delivery systems for future clinics. *Nanomedicine: Nanotechnology, Biology and Medicine* 2016; 12:143-161.

Bentz AB. Review of quercetin: chemistry, antioxidant properties, and bioavailability. *Journal of Young Investigators* 2009.

Crowley M, Feng Z, Martin C, et al. Pharmaceutical applications of hot-melt extrusion: part I. *Drug Development & Industrial Pharmacy* [serial online]. September 2007;33(9):909-926. Available from: Business Source Complete, Ipswich, MA. Accessed March 27, 2017.

Dan N. Compound release from nanostructured lipid carriers (NLCs). *Journal of Food Engineering* 2016; 171:37-43.

Dhawan S, Kapil R, Singh B. Formulation development and systematic optimization of solid lipid nanoparticles of quercetin for improved brain delivery. *Journal of Pharmacy and Pharmacology* 2011;63:342-351.

Douroumis D, Douroumis D. *Hot-Melt Extrusion: Pharmaceutical Applications*. Oxford: John Wiley & Sons, Incorporated; 2012.

Ehrlich SD. Quercetin. University of Maryland Medical Center. http://umm.edu/ health/medical/altmed/supplement/quercetin. Published October 19, 2015. Accessed March 27, 2017.

Flavonoids. Wako Laboratory Chemicals. http://www.wako-chem.co.jp/english/labchem/ product/life/Flavonoid/index.htm. Accessed March 27, 2017.

Gaudana R, Ananthula HK, Parenky A, Mitra AK. Ocular drug delivery. *The AAPS Journal*. 2010;12(3):348-360.

Harvard T.H. Chan. Antioxidants: beyond the hype. Available at: https://www.hsph.

harvard.edu/nutritionsource/antioxidants/#age-related%20eye%20disease%20 and%20antioxidants. Accessed March 27, 2017.

He Y, He Z, He F, Wan H. Determination of quercetin, plumbagin and total flavonoids in drosera peltata smith var. glabrata y.z.ruan. *Pharmacognosy Magazine*. 2012;8(32):263-267.

Hippalgaonkar K, Adelli GR, Hippalgaonkar K, et al. Indomethacin-loaded solid lipid nanoparticles for ocular delivery: development, characterization, and in vitro evaluation. *Journal of Ocular Pharmacology & Therapeutics* [serial online]. March 2013;29(2):216-228.

Kaufman PL, Alm A, Levin LA, et al. *Adler's Physiology of the Eye*. Philadelphia: Saunders; 2011.

Kelly GS. Quercetin. *Alternative Medicine Review* 2011;16:172-194.

Kumari A, Yadav SK, Pakade YB, et al. Development of biodegradable nanoparticles for delivery of quercetin. *Colloids and Surfaces B: Biointerfaces* 2010;80:184-192.

Mehnert W, Mäder K. Solid lipid nanoparticles: production, characterization and applications. *Advanced Drug Delivery Reviews* 2012; 64:83-101.

National Cancer Institute. Antioxidants and cancer prevention. Available at: https://www.cancer.gov/about-cancer/causes-prevention/risk/diet/antioxidants-fact-sheet. Accessed March 27, 2017.

National Eye Institute. All vision impairment. Available at: https://nei.nih.gov/eyedata/vision_impaired#1. Accessed March 27, 2017.

National Eye Institute. Prevalence of adult vision impairment and age-related eye diseases in america. Available at: https://nei.nih.gov/eyedata/adultvision_usa. Accessed March 27, 2017.

National Eye Institute. Vision impairment tables. Available at: https://nei.nih.gov/eyedata/vision_impaired/tables. Accessed March 27, 2017.

Prunty MC, Aung MH, Hanif AM, et al. In vivo imaging of retinal oxidative stress using a reactive

oxygen species–activated fluorescent probe. *Investigative Ophthalmology & Visual Science*. 2015;56(10):5862-5870.

Quercetin (ab120247). Abcam. http://www.abcam.com/quercetin-ab120247.html. Accessed March 27, 2017.

Quercetin [product insert]. Ann Arbor, MI: Cayman Chemical Company; 2016.

Repka MA, Battu SK, Upadhye SB, et al. Pharmaceutical applications of hot-melt extrusion: part II. *Drug Development & Industrial Pharmacy* [serial online]. October 2007;33(10):1043-1057.

Salunkhe VR, Patil SJ. UV spectrophotometric and hplc method development of quercetin and curcumin in polyherbal churna and its validation. *International Journal of Pharmaceutical and Phytopharmacological Research* n.d.;n.v.:1-16.

Srirangam R, Hippalgaonkar K, Avula B, Khan I, Majumdar S. Evaluation of the intravenous and topical routes for ocular delivery of hesperidin and hesperetin. *Journal of Ocular Pharmacology and Therapeutics* [serial online].2012; 28(6):618-627.

United Mitochondrial Disease Foundation. What is mitochondrial disease?. Available at: https://www.umdf.org/what-is-mitochondrial-disease/. Accessed March 27, 2017.

Weingerl V. A comparative study of analytical methods for determination of polyphenols in wine by hplc/uv-vis, spectrophotometry and chemiluminometry . In: *Macro to Nano Spectroscopy*. Croatia: InTech; 2012:357-370.

Wu TH, Yen FL, Lin LT, et al. Preparation, physicochemical characterization, and antioxidant effects of quercetin nanoparticles. *International Journal of Pharmaceutics* 2008.;346:160-168.